Swiss Journal of Geosciences (2018) 111:399–416
https://doi.org/10.1007/s00015-018-0302-y

Evaluating igneous sources of the Taveyannaz formation in the Central Alps by detrital zircon U–Pb age dating and geochemistry

Gang Lu[1] · Wilfried Winkler[1] · Meinert Rahn[2] · Albrecht von Quadt[3] · Sean D. Willett[1]

Received: 31 October 2017 / Accepted: 8 February 2018 / Published online: 23 February 2018

Abstract

Late Palaeogene syn-tectonic volcanic products have been found in the Northern Alpine foreland basin and in the South Alpine hemipelagic basin. The source of abundant volcanic fragments is still in debate. We analyzed the geochronology and geochemistry of detrital zircons, and evaluated their temporal and genetic relationships with potential volcanic sources. The study shows that the detrital zircon U–Pb age patterns have two major age groups: a dominance (ca. 90%) of pre-Alpine zircons was found, as commonly observed in other Alpine flysch formations. These zircons apparently derived from erosion of the early Alpine nappe stack in South Alpine and Austroalpine units. Furthermore, a few Neo-Alpine zircons (ca. 10%) have ages ranging from Late Eocene to Early Oligocene (~ 41–29 Ma). Both source materials were mixed during long riverine transport to the basin margins before being re-deposited by gravity flows. These Palaeogene ages match with the activity of Peri-Adriatic magmatism, including the Biella volcanic suite as well as the Northern Adamello and Bergell intrusions. The values of REE and $^{176}Hf/^{177}Hf_{(t)}$ ratios of the Alpine detrital zircons are in line with the magmatic signatures. We observe an in time and space variable supply of syn-sedimentary zircons. From late Middle Eocene to Late Eocene, basin influx into the South Alpine and Glarus (A) basins from the Northern Adamello source is documented. At about 34 Ma, a complete reorganisation is recorded by (1) input of Bergell sources into the later Glarus (B) basin, and (2) the coeval volcaniclastic supply of the Haute-Savoie basin from the Biella magmatic system. The Adamello source vanished in the foreland basin. The marked modification of the basin sources at ~ 34 Ma is interpreted to be initiated by a northwestern shift of the early Alpine drainage divide into the position of the modern Insubric Line.

Keywords North Alpine foreland basin · Flysch · LA-ICP-MS · Zircon Hf isotope · Palaeogeography

1 Introduction

Volcanic products of Middle Eocene to Early Oligocene age were distributed over a large area of the growing Alpine orogen including coeval outer and inner foreland basins, and the hemipelagic South Alpine basin. Generally, volcaniclastic sources along the Peri-Adriatic Line, in the Adamello, Bergell and Biella magmatic systems are regarded as sources by various authors. In the present study we focus on both the Northern Alpine Foreland Basin (NAFB) (North Helvetic Flysch, Taveyannaz Formation, TF) and the so-called Plagioclase Arenites (PA) in the Trentino Basin. Occurrences of the TF deposited in the northern underfilled foreland basin were investigated in the Glarus Alps, the Alpe Taveyanne and the Haute-Savoie areas (Fig. 1). Based on petrological, sedimentological and geochronological evidence, earlier studies attested strong influx of volcaniclastic detritus to the basins (e.g., Vuagnat 1944; Siegenthaler 1974; Lateltin and Müller 1987; Lateltin 1988; Sinclair 1992; Waibel 1993; Rahn 1994; Sciunnach and Borsato 1994; Ruffini et al. 1997; Boyet et al. 2001; Di Capua and Groppelli 2015). This view was corroborated by radiometric dating (K/Ar and Ar/Ar, hornblende) on single volcanic pebbles in the range of

Editorial handling: S. Spezzaferri.

Electronic supplementary material The online version of this article (https://doi.org/10.1007/s00015-018-0302-y) contains supplementary material, which is available to authorized users.

✉ Gang Lu
gang.lu@erdw.ethz.ch

[1] Geological Institute, ETH Zurich, Sonneggstrasse 5, 8092 Zurich, Switzerland

[2] Swiss Federal Nuclear Safety Inspectorate ENSI, Industriestrasse 19, 5200 Brugg, Switzerland

[3] Institute for Geochemistry and Petrology, ETH Zurich, Clausiusstrasse 25, 8092 Zurich, Switzerland

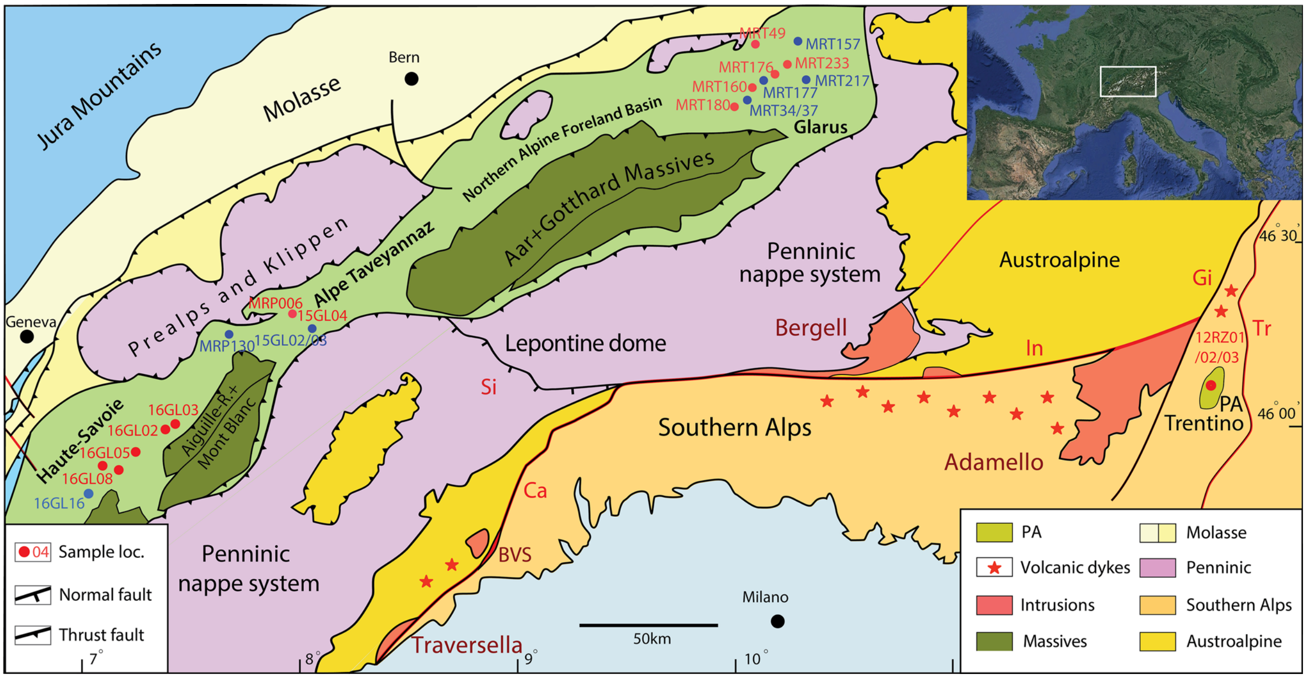

Fig. 1 Simplified tectonic map of the Central and Southern Alps with sample locations (Pfiffner 2014). Sample locations in red provided Palaeogene detrital zircons (blue-non). *BVS* Biella volcanic suite, *Gi* Giudicarie Line, *In* Insubric Fault, *Si* Simplon Fault, *Ca* Canavese Line, *Tr* Trentino Line, *PA* Plagioclase Arenites

~ 35–30 Ma (Fontignie et al. 1982; Fischer and Villa 1990; Féraud et al. 1995; Ruffini et al. 1997). However, the derivation and distribution of the volcanic material are still poorly defined.

Various hypothesis about their provenance were proposed. It is suggested that the volcaniclastic detritus was supplied from high-K igneous activity, which occurred in the internal part of the growing Alpine belt along the Peri-Adriatic Line, such as andesitic dykes, plutons and lava flows (Ruffini et al. 1997). Féraud et al. (1995) and Boyet et al. (2001) proposed the erosion of volcanoes located near or in the sedimentary Dauphinois-Helvetic flysch basin (outer foreland basin) as additional source. Similarly, according to Pfiffner (2014), the volcanic feeder dykes were more likely located in the southernmost part of the Aar massif, now beneath the Gotthard nappe, and thus not accessible at the surface. More recently, Di Capua and Groppelli (2015) interpreted the presence of primary volcanic deposits (pyroclastic density currents, PDC) or eruption-triggered flow deposits (their facies type 3) as sedimentary response to the magmatic activity along the Peri-Adriatic volcanic belt.

With regard to the Plagioclase Arenite deposits in the Trentino basin the source-to-sink situation appears simpler. Within the Giudicarie fault zone Eocene turbiditic, plagioclase-rich intercalations in pelagic sediments (Ponte Pià Fm. were identified by Bars and Grigoriadis (1969) and Sciunnach and Borsato (1994), respectively. Petrologic, geochemical analyses and a radiometric age (zircon U–Pb, 35.4 Ma) support the derivation of the volcaniclastic material from extrusions and dykes related to the Adamello magmatic system (Martin and Macera 2014). The results from this well established source-to-sink relationship will serve as an important correlation tool in the present study.

In summary, various potential detrital volcanic sources could hardly be discriminated in earlier works. In addition, our observations suggest that the TF bears also variable and high amounts of siliciclastic grains probably derived from continental basement rocks in the source areas, which was virtually neglected by earlier investigators. This mixing of old basement and minor contemporaneous detritus calls à-priori for a long distance riverine transport to the NAFB margin.

Our approach for revealing the provenance of clastic material in general, and in particular their relationship to orogenic intrusive and eruptive episodes, is to systematically apply detrital zircon analysis. We analyse U–Pb dates of detrital zircons (DZ) from sandstones by laser ablation inductively coupled plasma mass spectrometry (LA-ICP-MS) (see e.g., Gehrels 2014, for the wide field of applications). Additionally, trace element contents (REE) and in situ Hf isotope analyses (e.g., Belousova et al. 2002; Hawkesworth and Kamp 2006) are performed on those zircons, which by age correlate with Palaeogene Alpine magmatic activity. We expect to discriminate between the different Peri-Adriatic magmatic systems as sources. The unexpectedly high abundance of reworked basement material in the TF and its derivation, and the possible existence of additional volcaniclastic sources closer to the basin, i.e. along the southern margin of the NAFB (North Helvetic Flysch) depositional site will be also discussed.

2 Geological framework

The Late Palaeogene sedimentary sequence of the NAFB is formed in the course of the continent–continent collision during the Alpine orogeny (e.g., Trümpy 1973). The basin is characterized by an initial underfilled 'flysch stage' of Late Eocene-Early Oligocene age (e.g., Allen et al. 1991; *Sinclair* 1992). The resulting turbidite-dominated series were deposited within the inner deformed margin of the foreland basin in a wedge-top position (DeCelles and Giles 1996) and are attributed to the North Helvetic Flysch. This flysch extends in a narrow band ($\sim$ 15 km width) over 200 km from the Subalpine chain in the Haute-Savoie to the Glarus area in the east (Fig. 1). The lower stratigraphic boundary of the basin series is marked by a major unconformity, which is known as the 'Palaeocene Restoration' (Trümpy 1973). The unconformity separates the eroded underlying Mesozoic northern continental margin succession from the overlying Palaeogene foreland basin sediments, which show a marine deepening trend. This particular tectono-stratigraphic configuration was driven by earlier foreland bulge uplift (starting in latest Cretaceous) followed by progressive stratigraphic onlap of the foreland basin fill during flexural subsidence (Allen et al. 1991; Sinclair 1992).

The Plagioclase Arenites in the western Southern Alps (Trentino basin) (Fig. 1) were deposited in a completely different environment, namely in a hemipelagic basin of outer neritic to bathyal depth (Sciunnach and Borsato 1994). Outcrops are located in the Giudicarie belt separating the Lombardy basin to the west from the Trentino basin in the east (Doglioni and Bosellini 1987). A volcaniclastic source of the sandstones intercalated into hemipelagic/pelagic marl- and limestones from extrusions and dykes related to the Adamello magmatic system is presently accepted (Sciunnach and Borsato 1994; Castellarin et al. 2005; Martin and Macera 2014).

3 Stratigraphy and lithology

3.1 Glarus, Alpe Taveyanne and Haute-Savoie

The TF, traditionally considered as a turbidite sandstone series rich in volcanic debris, has its main occurrence in the Glarus area below the Glarus thrust, in the type locality Alpe Taveyanne and the Haute-Savoie in France. The Grés de Chaupsaur Fm. represents their closest stratigraphic continuation to the southwest in France, at the southern margin of the Pelvoux massive (e.g., Boyet et al. 2001) (not shown in Fig. 1). In the eastern NAFB in Austria (NE of Salzburg) coeval sandstone formations ("Rupelian" sandstones) document volcaniclastic input (Sharman et al. 2017). The strong folding and internal thrusting as well as very low-grade metamorphic overprint, especially in the Glarus section (e.g., Rahn et al. 1995; Ferrero Mählmann 1995), hampered until now precise biostratigraphic correlations.

In the studied sections of the NAFB a similar stratigraphic subdivision (Fig. 2) is generally accepted comprising the underlying deepening-upward series of the Einsiedeln and Stad formations. They are also informally known as Nummulitic limestones and *Glogiberina* marls, respectively (Stratigraphic Lexicon of Switzerland, https://www.strati.ch). Presumably diachronously (Lateltin 1988) follows the TF. Scarce nannoplankton data (Lateltin 1988) indicating NP 21-23 correlate the formation with the latest Eocene (Priabonian)-Early Oligocene (Rupelian) in western Switzerland and France. However, the range of the present DZ U–Pb datings from the Glarus area could allow establishing a maximum older age in the Bartonian if transport and resedimentation of grains is considered geologically rapid in the range of several 100 kys. In the Alpe Taveyanne and Haute-Savoie our DZ age results confirm the biostratigraphic correlation of Lateltin (1988).

The Taveyannaz Fm. consists of green turbiditic sandstone and dark-grey shale layers of variable thickness (Fig. 3) and totals several hundred meters. On microscopic scale it shows poorly sorted and often zoned volcanogenic feldspars, andesitic fragments and a small amount of mafic minerals. The andesitic grains are in variable amounts mixed with quartz, feldspar, calcite, white mica and metamorphic fragments. Furthermore, in the Glarus section, based on our radiometric dating of DZ (see below) we may distinguish two informal members, an older member A and a younger member B. Observed lithological and sedimentological similarities in the context of intensive fold deformation in Glarus do not exclude the possibility that our sample and data set also includes sandstones from the Elm and Matt fms.

The TF is topped by continued turbidite deposition represented by the Elm and Matt fms. in central Switzerland, and the Grés du Val d'Illiez in western Switzerland and France, respectively. Both formations terminate the underfilled stage of the NAFB.

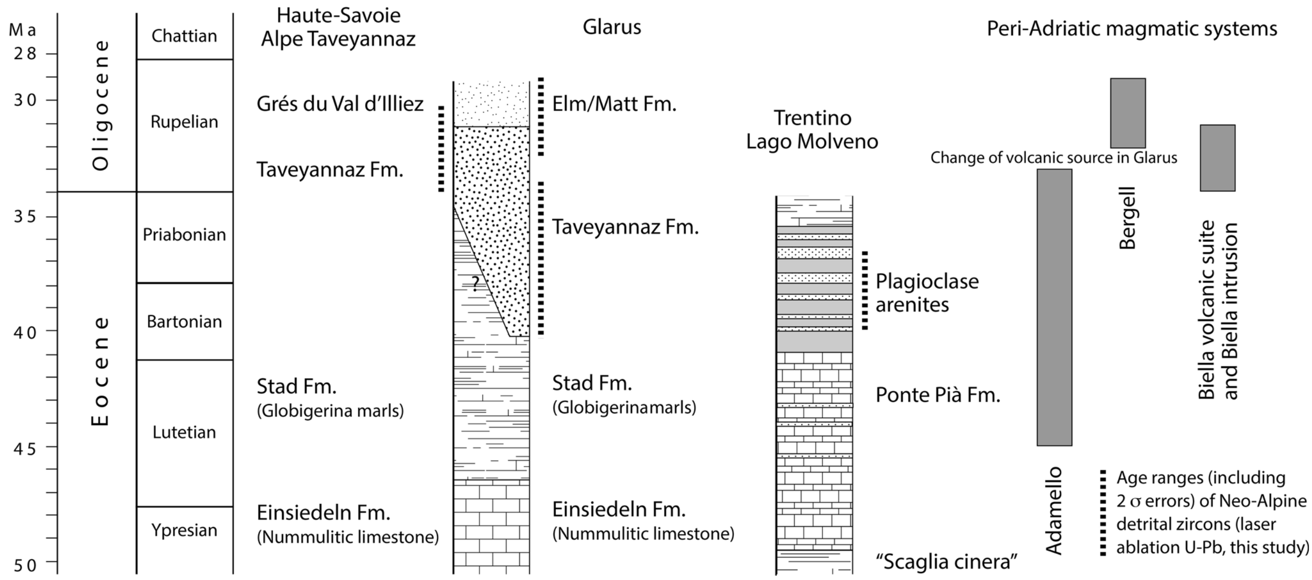

Fig. 2 Composite stratigraphy of the Palaeogene sections studied in the North Alpine foreland basin (North Helvetic Flysch) and Southern Alps (Trentino Basin) in comparison with age ranges of the Peri-Adriatic intrusions Compiled from Siegenthaler (1974), Pfiffner (1986), Sinclair (1992), Sciunnach and Borsato (1994), Zurfluh (2012). Time scale after Gradstein et al. (2012)

3.2 Trentino basin

Sciunnach and Borsato (1994) evaluated a Late Eocene age (latest Bartonian-Priabonian) based on nannoplankton and planktonic foraminifera. The Plagioclase Arenites (PA) conformably overly the hemi-pelagic Ponte Pià Fm. comprising bedded limestones occasional fine sandstones and bioturbated marlstones with increasing amount of marlstones towards the top. In the upper part of the formation and below calcarenitic turbidite layers bentonites are observed (Zurfluh 2012). The PA do not have a formal lithostratigraphic rank but were considered as a special facies in the Ponte Pià Fm. They represent irregular intercalations of turbidite beds of dm-scale thickness, the most prominent one with a thickness of $\sim$ 3 m occurs in the Lake Molveno area (Sciunnach and Borsato 1994).

4 Late Alpine calc-alkaline magmatism

The syn-collisional magmatism along the Peri-Adriatic fault system consists of calc-alkaline and shoshonitic suites with mainly granodioritic, tonalitic intrusions and andesitic volcanism (e.g., Waibel 1993; Rosenberg 2004; Pfiffner 2014). Due to strong deformation during the Neogene, it is difficult to reconstruct its volume and geometry. The calc-alkaline magmatism is linked to Alpine convergence, but its exact origin is still a matter of debate: continental arc, product of the collision detachment of a lithospheric panel, or back-arc extension (e.g., von Blankenburg and Davies 1995; Beltrando et al. 2010; Pfiffner 2014). A widely accepted model for the late Alpine magmatism along the Peri-Adriatic fault system is the oceanic slab break-off model inferred by von Blanckenburg and Davies (1995). This process may have driven mantle upwelling and heat transport giving rise of intensive magmatic activity and rapid exhumation of the plutonic bodies. The three most important volcanic/plutonic suites and potential sources for detrital zircons in the TF are shortly characterised in the following.

4.1 Biella volcanic suite (BVS), Valle de Cervo and Miagliano plutons

Today, the BVS is restricted to a narrow belt about 20 km along the Canavese line in the Sesia–Lanzo zone (Fig. 1). The composition of the volcanic rocks ranges from basalt to andesite in the high-K calc-alkaline suite and from trachyandesite to trachydacite in the shoshonitic suite (Callegari et al. 2004). The BVS represents a complex volcanic sequence of porphyries, coarse-grained conglomerates, volcanic breccias and thin tuffitic layers. Based on palaeobotanical data and K–Ar total rock ages of andesitic rocks, Scheuring et al. (1974) assessed an age of volcaniclastic rocks between 29 and 33 Ma. More recently, Kapferer et al. (2012) measured U–Pb zircon ages at 32.89–32.44 Ma for the eruption of the cal-alkaline lavas. By high precision zircon U–Pb dating, from the Biella intrusion Berger et al. (2012) achieved an age of 33.00 $\pm$ 0.04 Ma for the central tonalitic part of the Miagliano pluton and 30.39 $\pm$ 0.50 Ma for the granitic core of the Valle del Cervo pluton. In a tentative estimate, the

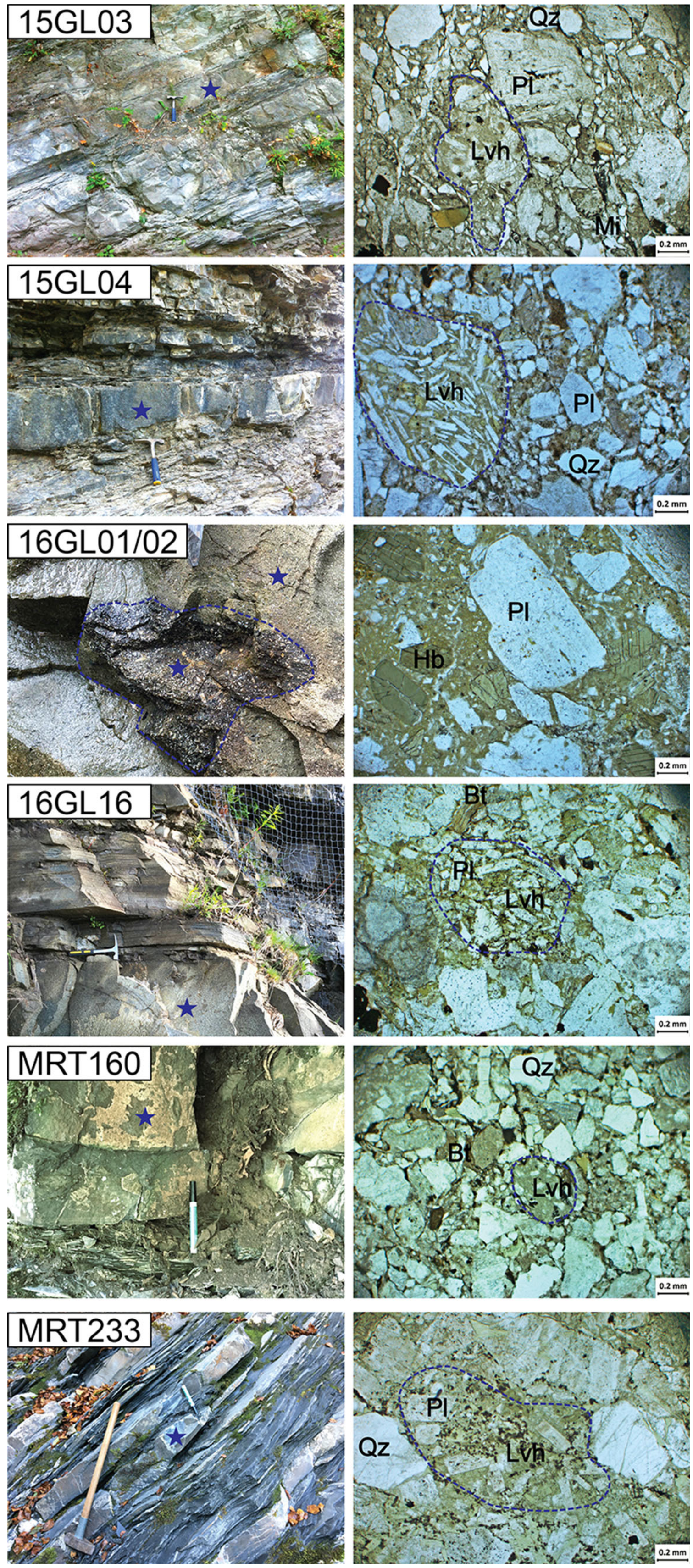

Fig. 3 Sample location (red stars) and microphotographs (plain light) of analysed sandstones. *Qz* quartz, *Pl* plagioclase, *Hb* hornblende, *Mi* white mica, *Bt* biotite, *Lvh* volcanic hypabyssal lithoclast

Biella intrusion and volcanics can be correlated with 34–31 Ma.

4.2 Bergell intrusion

The intrusion is located in the SE of the Alpine orogenic belt and today covers a surface area of approximate 50 km^2. The pluton is nearly concentrically zoned, exposing granodiorite in the core and tonalite at the margin. The southern tail of the Bergell pluton is a 40 km long steep tabular body of tonalite, which formed due to right-lateral movement along the Peri-Adriatic fault. Post-intrusive tilting and exhumation resulted in the exposure of a 12 km deep crustal section (Rosenberg 2004). Zircon and allanite U–Pb (Th–Pb) ages from the Bergell intrusion range from 33 to 29 Ma (e.g., von Blankenburg 1992; Gianola et al. 2014; Tiepolo et al. 2014).

4.3 Adamello batholith

The Adamello batholith forms the largest intrusive complex in the Alps (e.g., Pfiffner 2014). Its internal part is crossed only by a few late- to post-magmatic fault zones (Callegari and Brack 2002; Schaltegger et al. 2009). Adamello magmas were emplaced from Middle/Late Eocene to Early Oligocene. From northeast to southwest the entire batholith can be subdivided into four different plutonic bodies: Presanella, Avio, Adamello and Re di Castello. The individual plutons are composite bodies displaying varying structural relationships among each other and their adjacent rocks (Rosenberg 2004). They were emplaced over a period of around 9 Myr, successively from the oldest units in the southwest ($\sim$ 42 Ma) to the youngest in the northeast ($\sim$ 33 Ma) (e.g., Mayer et al. 2003; Schaltegger et al. 2009; Schoene et al. 2012; Skopelitis et al. 2011; Skopelitis 2014).

5 Sample materials

5.1 Sandstones

Our analyses are based on sandstone samples collected from various sections in Switzerland, France and Italy (Table 1). Earlier authors have systematically evaluated the modal composition of these sandstones except in the Glarus area. The sandstones of the TF of Haute-Savoie and Alpe Taveyanne area are subarkosic to lithoarenitic (Lateltin 1988; Lateltin and Müller 1987; Di Capua and Gropelli 2015). Selected examples of outcrop and microscopic views are given in Fig. 3. The sandstones are normally (rarely inveresly) graded turbidites and are greenish-brown in colour. Grain size variies from medium to coarse, sporadically also containing out-size pebbles. Typically, the sandstones also bear rip-up clasts (mud-chips). In thin sections, volcanic lithoclasts are largely dominating whereas continental basement and sedimentary lithoclasts are rarer. Plagioclase is a further abundant grain type, pyroxene, amphibole and biotite occur in minor proportions. However, the variable presence of quartz grains (from $< 10\%$ up to 50%) imply the incidence of basement erosion in the hinterland. This is also supported by variable amounts of white mica. In the Gres de Val'Illiez a further increase of quartz (to values $> 60\%$, Lateltin 1988) and white micas is obvious. A similar increase of quartz grains and white micas in the Elm and Matt fms. was also reported from the Glarus area (Siegenthaler 1974).

The Plagioclase Arenites from the Southern Alps (Trentino basin) are classed as arkoses with a virtual lack of quartz and minor rates of volcanic rock fragments (Zurfluh 2012). The sandstone is dark green with gray and black minerals.

It contains abundant weathered plagioclase with average size of about 0.25 mm. Partly, the plagioclase was converted to chlorite and sometimes replaced by calcite from the centre. An analysis of translucent heavy minerals by the same author revealed prevailing apatite ($> 50\%$), zircon and biotite ($\sim$ 20% each), hornblende ($\sim$ 5%) and sporadic garnet, anatase and epidote. Hence, the sandstones represent typical volcanic arenites virtually missing basement rock influx.

5.2 Volcanic pebbles in the Glarus area

In the Sernftal area a peculiar kind of volcanic pebbles was documented by Siegenthaler (1974). The pebbles represent several cm-sized clasts enclosed in the sandy turbiditic matrix deposited by highly concentrated gravity flow deposits (Fig. 4). After textural and mineralogical criteria we distinguish three types of pebbles:

Type 1: altered hornblende + plagioclase replaced by calcite + sparry calcite + chloritic matrix + opaques (Fig. 4a),

Type 2: plagioclase replaced by calcite in a chloritic matrix (Fig. 4b),

Type 3: plagoclase partially replaced by calcit + sparry calcite cement (also poikilotopic) (Fig. 4c). Figure 4d shows a pebble-in-pebble configuration of type 2 and 3.

In the pebbles the original magmatic texture is well preserved. The above listed alterations (replacements) causing calcite growth and chloritic matrix document strong post-magmatic alteration most likely in an aquatic environment as described by e.g., Gifkins et al. (2005) or Shanks (2012) and we suggest that the pebbles represent metasomatic products of primary andesitic flows entering an aquatic environment. Their fragile mineralogical

Table 1 Location and description of analysed samples from the North Alpine foreland basin (North Helvetic Flysch) and Southern Alps (Trentino basin)

Area	Locality	Latitude	Longitude	Longitude/latitude swiss grid	Altitude (m)	Sample
Haute-Savoie	Flaine	46°0′36″N	6°40′40″E	541 064/95 670	1840	16GL02
		46°0′46″N	6°41′08″E	541 669/95 973	1990	16GL03
	Col de l'Oulette	45°57′50″N	6°32′02″E	529 860/90 663	1930	16GL05
	Chalêt des Juments	45°53′39″N	6°26′26″E	522 526/83 000	1500	16GL08
	Bois de Molliettes	45°52′48″N	6°20′60″E	515 475/81 519	980	16GL16
Alpe Taveyanne region	Val d'Illiez	46°12′53″N	6°54′57″E	559 650/118 260	1000	MRP 130
	Lizerne	46°14′47″N	7°15′18″E	585 836/121 678	1170	15GL02
	Lizerne	46°14′4″N	7°15′20″E	585 876/120 350	1180	15GL03
	Alpe Taveyanne	46°18′ 4″N	7°07′33″E	575 935/127 780	1780	MRP 006
		46°18′ 5″N	7°7′34″E	576 920/127 824	1790	15GL04
Glarus B	Wageten	47°07′ 6″N	9°00′18″E	717 790/219 400	1610	MRT 049
		47°08′23″N	9°06′10″E	726 240/222 300	490	MRT 157
	Luchsingen	46°58′ 1″N	9°01′55″E	721 240/203 000	640	MRT 160
	Luchsingen	46°58′34″N	9°03′27″E	723 170/204 050	640	MRT 177
Glarus A	Elm	46°58′03″N	9°10′17″E	731 850/203 280	890	MRT 217
	Linthal	46°55′32″N	9°00′44″E	719 850/198 360	730	MRT 034
		46°55′32″N	9°01′07″E	720 326/198 373	1020	MRT 037
		46°54′43″N	8°59′04″E	717 750/196 800	760	MRT 180
	Luchsingen	46°56′49″N	9°01′51″E	721 380/200 790	660	MRT 176
Trentino	Schwanden	46°59′47″N	9°05′31″E	725 750/206 360	560	MRT 233
	Lago di Molveno	46°07′51″N	10°58′21″E	873 036/114 967	200	12RZ01/02

content and the infiltration of host sand (Fig. 4c) argues for a short transport from a volcanic source nearer as others. According to Siegenthaler's (1974) lithostratigraphy, these pebbles occur in the locally called Ruchi Sandstone, the uppermost member of the TF.

6 Results

6.1 Detrital zircon U/Pb ages

As evident from cathodoluminescence pictures (Fig. 5), zircon grains from the TF are mainly prismatic fragments or euhedral crystals. Only a few sub-rounded and unzoned grains were found. The large majority of the zircons show well-developed oscillatory zoning and inherited cores recording older geological events. The internal features indicate a magmatic origin (Rubatto and Gebauer 2000).

The age distribution of detrital zircons reveals a large dominance (> 90%, of total 1500 dated zircons) of pre-Alpine ages as commonly observed in other Alpine flysch formations (e.g., Bütler et al. 2011; Beltràn et al. 2013). The following age clusters consistent with older orogenic cycles comprised in the Alpine basement can be idntified (Fig. 6): (1) Cadomian (650–540 Ma) with an amount of ~ 10% of the total. The major peak lies at 582 Ma, (2) Caledonian (497–393 Ma) U/Pb ages contribute ~ 45% to the major peak at 452 Ma, and (3) Variscan and post-Variscan (393–252 Ma) zircons represent about 35% with major peaks at around 290 and 270 Ma. There is no quantitative difference of the pre-Alpine zircon age populations observed at the presence or lack of Palaeogene zircons (Fig. 6).

Palaeogene detrital zircons (< 10%, of the total 1500 dated zircons) range from ~ 41 to ~ 29 Ma. Six samples from the Haute-Savoie and Alpe Taveyanne area yielded a total of 11 consistent ages ranging from ~ 30–34 Ma including two sigma errors (Fig. 7). In the Glarus area two distinct age populations, derived from different sandstones, are identified: ~ 41–32 and ~ 33–29 Ma. Hereafter we refer to them as Glarus A (older age range) and Glarus B members (younger age range). Similar to Glarus A, the South Alpine Trentino sandstones (Plagioclase Arenites) reveals consistent ages of ~ 41-33 Ma.

6.2 Rare earth elements

REE signatures of Alpine DZ from the TF in the various occurrences are here compared with published zircon REE data (Northern Adamello and Bergell intrusion data from

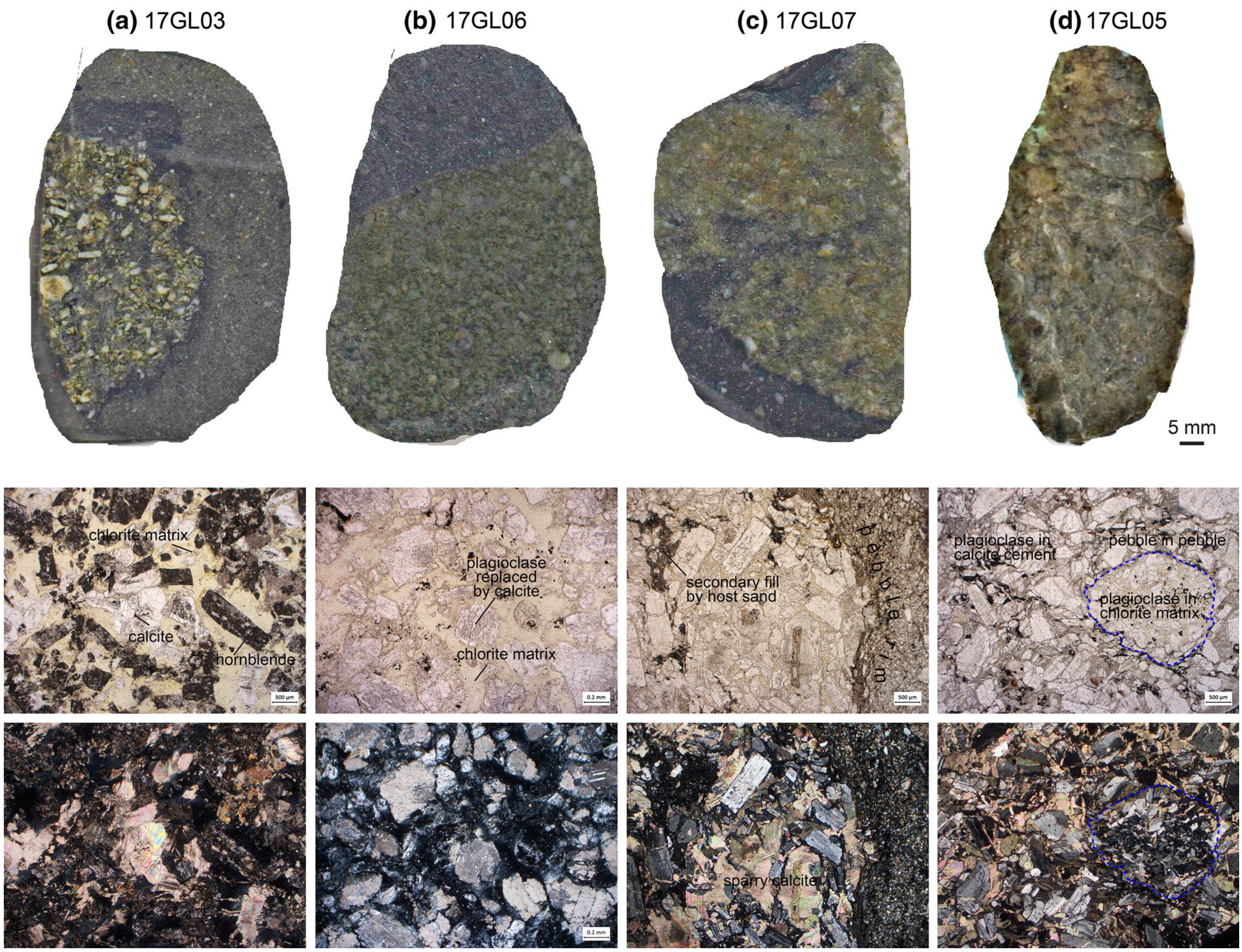

Fig. 4 Rock slab and thin section photographs (plain and polarised light) of phreato-volcanic pebbles in the Glarus B Taveyannaz Fm. (Ruchi sandstone after Siegenthaler 1974). **a** 17GL03 (type 1); **b** 17GL06 (type 2); **c** 17GL07 (Type 3); **d** 17GL05 (pebble in pebble, type 2 in type 3)

Rossetti et al. 2007; Broderick et al. 2015; Gianola et al. 2014). All show that the Alpine DZ from different volcanic sources have slightly different geochemical signatures (Fig. 8). Normalized zircon trace element patterns display enrichment relative to CI-chondrites (McDonough and Sun 1995). The REE patterns are characterized by a positive Ce anomaly ($Ce_N/Ce^* = 26.2–353.6$, $Ce^* = (La_N{*}Pr_N)^{1/2}$), characteristic for oxidizing environment, as a result of the preferential incorporation of Ce^{4+} (instead of Ce^{3+}) in zircons (Schaltegger et al. 2009). Furthermore, all zircon grains from the TF have chondrite-normalized REE patterns enriched in HREE. A slight difference in the values of εEu ($Eu_N/Eu^* = Eu^*2/(Sm + Gd)$, ~ 0.1-0.9) suggests the diversity of the magma source during the crystallization of zircons (Fig. 9a). Combined with the zircon REE data (Fig. 8), it indicates that zircons in the Glarus A TF and the Plagioclase Arenites overlap with primary zircons of the Adamello magmatic system. Similarly, the zircons of Glarus B and Haute-Savoie TF reveal a close correlation with Bergell and Biella, respectively.

6.3 $^{176}Hf/^{177}Hf$ ratios

On Palaeogene zircon grains, initial $^{176}Hf/^{177}Hf$ ratios ($\varepsilon Hf_{(t)}$) were measured after zircon U/Pb age dating. The results reveal a clear clustering of the DZ with regard to ages and Hf isotopic signatures (Fig. 9b). Late Middle Eocene to Late Eocene zircons from the Glarus A TF yield negative values of εHf (− 1.6 to − 5.6). Early Oligocene (Rupelian) Glarus B TF zircons reveal positive values of εHf (+ 4.1 to + 7.8). Rupelian (34.2–30.2 Ma) TF zircons in the Haute-Savoie area disclose negative values of εHf (− 1.2 to − 5.7). A similar overlap pattern as in εEu values is observed.

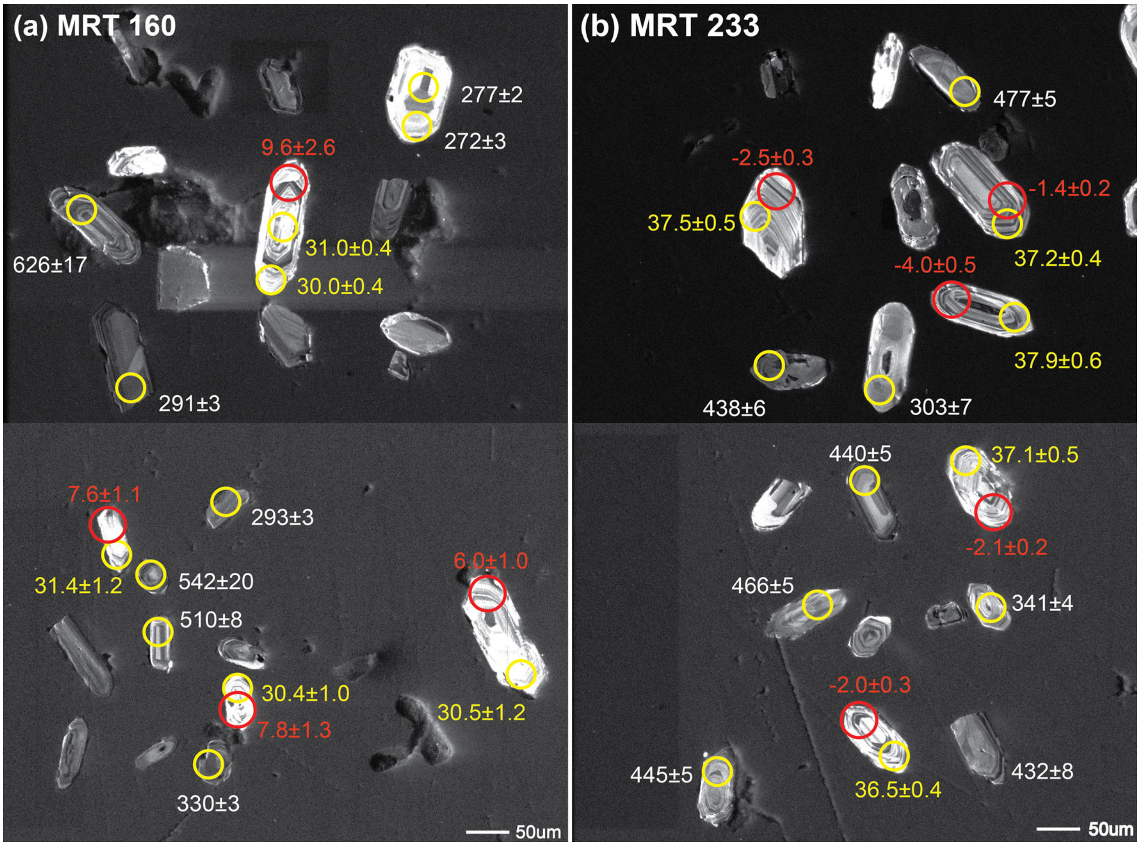

Fig. 5 Cathodoluminescence images of zircon grains in the TF (**a**: MRT 160, **b**: MRT 233), showing the spot of $^{206}Pb/^{238}U$ age (Ma, yellow lables and circles) and $^{176}Hf/^{177}Hf$ ratios (red lables and circles). Errors are 2σ

7 Discussion and interpretation

7.1 Synsedimentary volcanic sources

The DZ U–Pb age populations we measured in the TF from the various occurrences indicate massive reworking of Alpine crystalline basement units into the basins (Fig. 6). The observed prevalence of Neoproterozoic to post-Variscan zircons (> 90%) is certainly amplified by the known low production of zircons in andesitic magmatic eruptions as supposed for the volcanic sources of the TF. In addition, volcanic lithoclasts and associated zircons may also have been supplied by older volcanic units (e.g., Carboniferous, Permian) included in the sandstones, but microscopically indistinguishable. A dominance of syn-sedimentary volcanic products was generally inferred from the sandstone composition (e.g., Vuagnat 1944; Siegenthaler 1974; Lateltin 1988; Di Capua and Croppelli 2015), because several single andesitic pebbles and mineral concentrates could be dated with K/Ar and Ar/Ar methods in the range of 40-30.5 Ma (Fontignie et al. 1982; Fischer and Villa 1990; Ruffini et al. 1997; Féraud et al. 1995; Boyet et al. 2001) (Table 2). In-situ U–Pb age dating of DZ, however, provides a larger insight into the detrital source composition, especially the crystalline basement. In comparison with other central Alpine rift, drift and subduction (flysch) related sandstone formations (Buetler et al. 2011; Beltràn et al. 2013, 2016), synsedimentary volcanic material influx into the foreland basins is clear.

Finally, the obtained age ranges of DZ, REE values, Eu and Hf-isotope ratios vs. $^{206}Pb/^{238}U$ grain ages (Fig. 6, 7, 8, 9) allow to discriminate the volcanic contribution (1) to the Haute-Savoie/Alpe Taveyanne and Glarus B basins from the Bergell and Biella magmatic systems, respectively, and (2) the DZ age ranges and REE signatures in the Glarus A TF and the South Alpine Plagioclase Arenites flawlessly correlate with zircon U–Pb dates and REE patterns from the Northern Adamello batholith. However, volcanic products presumably related to Southern Adamello intrusions were not revealed in the TF.

The low resistant phreato-volcanic pebbles in the Glarus B Taveyannaz Fm. presumably represent local volcanic activity likely along the southern margin of the NAFB. The so-called telemagmatic dykes described by Furrer and Hügi (1952) in the Nummulitic limestones (Einsiedeln Fm.) of the central Helvetic nappes may represent passageways of the ascending magmas.

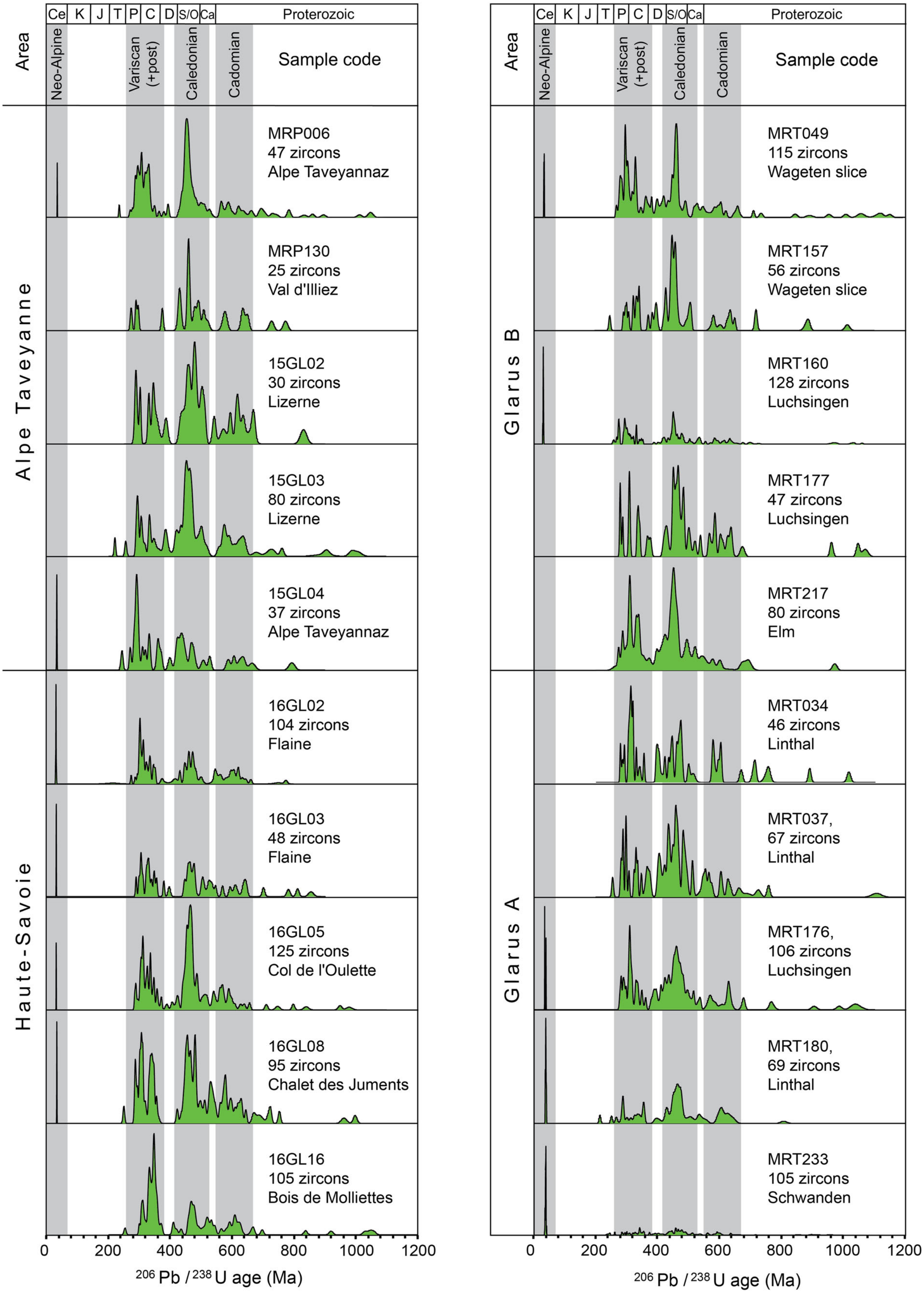
Ce K J T P C D S/O Ca Proterozoic
Area
Neo-Alpine
Variscan (+post)
Caledonian
Cadomian
Sample code
Alpe Taveyanne
MRP006
47 zircons
Alpe Taveyannaz
MRP130
25 zircons
Val d'Illiez
15GL02
30 zircons
Lizerne
15GL03
80 zircons
Lizerne
15GL04
37 zircons
Alpe Taveyannaz
Haute-Savoie
16GL02
104 zircons
Flaine
16GL03
48 zircons
Flaine
16GL05
125 zircons
Col de l'Oulette
16GL08
95 zircons
Chalet des Juments
16GL16
105 zircons
Bois de Molliettes
0 200 400 600 800 1000 1200
206 Pb / 238 U age (Ma)
Glarus B
MRT049
115 zircons
Wageten slice
MRT157
56 zircons
Wageten slice
MRT160
128 zircons
Luchsingen
MRT177
47 zircons
Luchsingen
MRT217
80 zircons
Elm
Glarus A
MRT034
46 zircons
Linthal
MRT037,
67 zircons
Linthal
MRT176,
106 zircons
Luchsingen
MRT180,
69 zircons
Linthal
MRT233
105 zircons
Schwanden

◀**Fig. 6** Probability U–Pb age curves of detrital zircon ages from sandstones of the Taveyannaz, Elm/Matt and Grés de Val d'Illiez formations. Only concordant ages are considered and also small error ellipses situated close and only below the concordant age curve (Ludwig 2009, ISOPLOT). Time scale after Gradstein et al. (2012)

7.2 Pre-Alpine basement sources

The U–Pb ages of detrital zircons show a wide age range from Permian to Precambrian, with three composite peaks (Cadomian, Caledonian, Variscan and post-Variscan)

Fig. 7 Compilation of Palaeogene detrital zircon U–Pb dating results compared with geochronological ages of the Peri-Adriatic intrusions (after Kapferer et al. 2012; Berger et al. 2012; Skopelitis et al. 2011; Skopelitis 2014; Tiepolo et al. 2014; Gianola et al. 2014). Age errors in 2σ

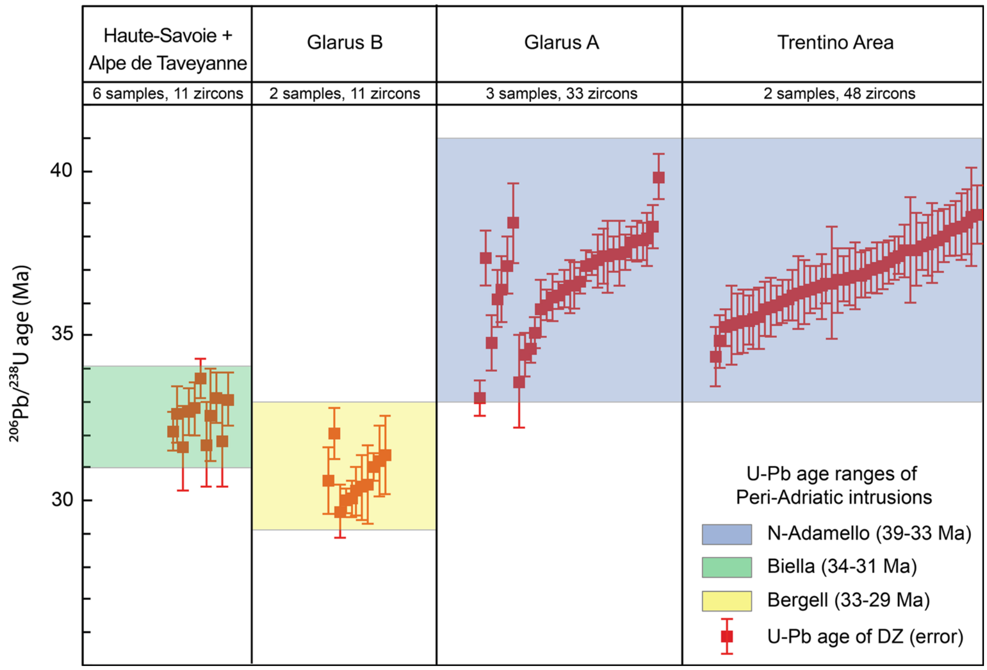

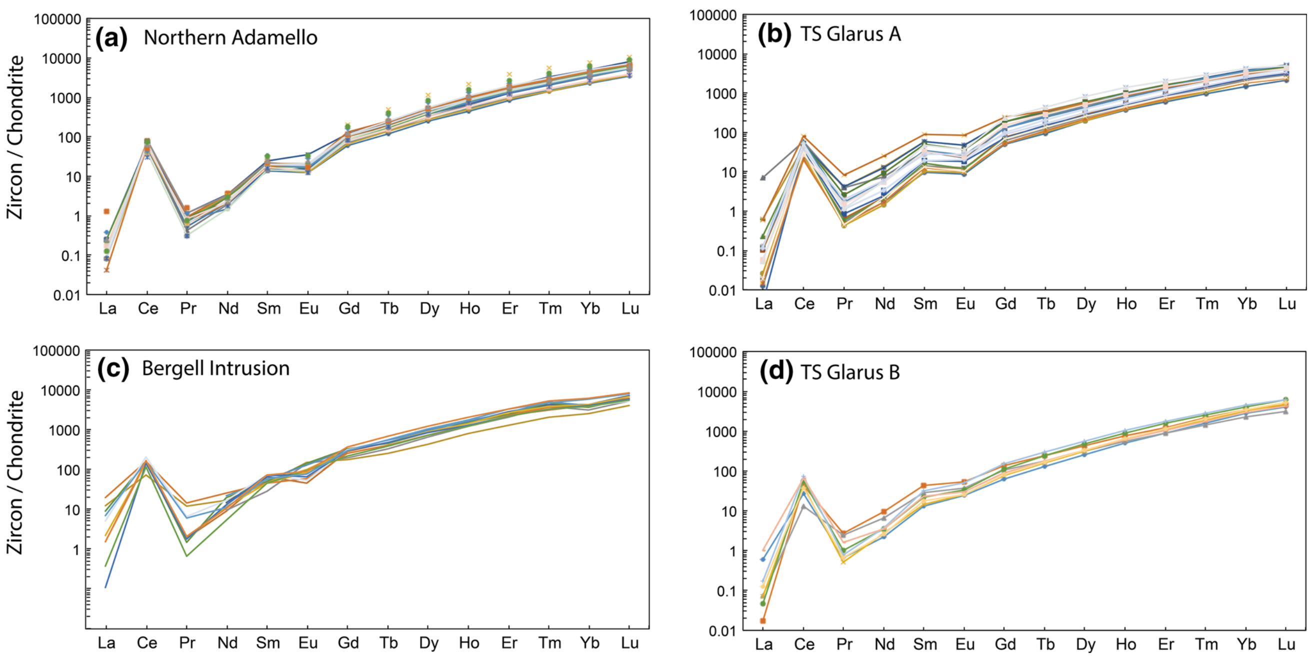

Fig. 8 Rare earth element patterns of detrital zircons from sandstone of Taveyannaz Fm (TS) compared with REE data from Peri-Adriatic magmatic rocks. Date sources: Northern Adamello (Skopelitis et al. 2011; Skopelitis 2014; Broderick et al. 2015), Bergell intrusion (Gianola et al. 2014). All diagrams are normalized to CI-chondrite (McDonough and Sun 1995)

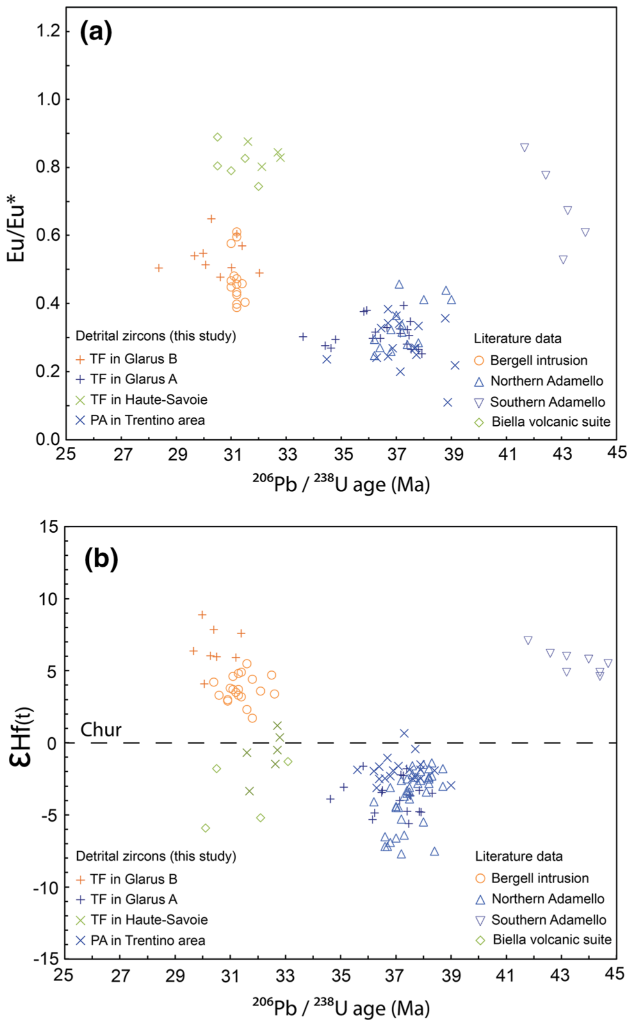

Fig. 9 **a** Epsilon Eu-ratios ($Eu_N/Eu^* = Eu^*2/(Sm + Gd)$) evaluated on U–Pb dated detrital zircons of the Taveyannaz Fm. compared with REE data from Peri-Adriatic magmatic rocks. **b**:Epsilon Hf-ratios evaluated on U–Pb dated detrital zircons of the Taveyannaz Fm. (TF) and Plagioclase Arenites (PA). Date sources: Skopelitis et al. (2011); Skopelitis 2014; Broderick et al. (2015); Ji et al. (2013); Stipp et al. (2013); Tiepolo et al. (2014); Gianola et al. (2014)

(Fig. 6). The following age clusters consistent with older orogenic cycles comprised in the Alpine basement can be identified: (1) the largest age group observed correlates with the Cadomian orogenic activity roughly between 650 and 550 Ma (Stern et al. 2004); (2) the Caledonian cluster (Cambrian, Ordovician, Silurian and Early Devonian) represents the second basement source. Ordovician rock series are also well documented within the Variscan basements of Alps (von Raumer et al. 2013). Frisch et al. (1984) explained the magmatic activity by Cambrian-Ordovician rifting that should have occurred along the northern Gondwana margin; (3) Variscan and post-Variscan age populations, ranging the Middle Devonian, Carboniferous and Permian, are consistent with the Variscan orogenic cycle with magmatic activity and metamorphism followed by post-Variscan extension between 333 and 268 Ma (e.g., Rubatto and Hermann 2003; von Raumer et al. 2013; Letsch et al. 2015).

7.3 Palaeogeographic reconstruction

Foreland basin development is controlled by a variety of factors, including flexural rigidity of the subducted plate, sedimentary load, orogenic load, forward migration of the orogenic front and orogenic uplift (e.g., Sinclair 1992; Ford and Lickorish 2004). In the NAFB the Late Eocene-Early Oligocene TF turbiditic sandstones grade up from Helvetic hemipelagic series (Stad Fm.). A formation of the basins in a wedge-top situation is inferred (Pfiffner 1986; Sinclair 1992; Sinclair and Tomasso 2002). Obviously, the basins were topographically confined as it could be reconstructed in the less deformed parts in the Haute-Savoie and Alpe Taveyanne areas. Lateltin (1988) and Di Capua and Cropelli (2015) suggested Turbiditic transport, parallel to the W-E oriented basin axis. With regard to the abundance of Alpine basement zircons and other crystalline rock indicators such as white mica and quartz grains, a broad area of the early Alpine basement nappe stack largely should have contributed to the basin debris. The transition from the hemipelagic Stad Fm. to the turbidite fan Taveyannaz Fm. implies a period of rapid uplift in the orogenic wedge and the development of river systems feeding deltas along the NAFB margin from late Middle Eocene. From a given time, the river catchments cut back into parts of the Per-Adriatic volcano-plutonic provenance. By considering such processes in a short period (i.e. in the range of a few Myr) we suggest that deposition of the TF in Glarus started considerably earlier, during Priabonian at the latest.

From our DZ U/Pb ages, stratigraphy and geographical basin relationships we suggest the following palaeogeographical model:

7.3.1 41–34 Ma (Bartonian-Priabonian, Fig. 10a)

During the early stage of sediment deposition, the Taveyannaz Fm. developed mainly in the Glarus area with turbiditic fan deposition in the Glarus A basin. The transition from hemipelagic (Stad Fm.) to turbiditic siliciclastic facies suggest strong uplift and exhumation in the hinterland during this period. Rivers drained the early Central Alpine basement and cover nappe stack and cut back into the Adamello magmatic system. In such a model, the water divide between the Central and Southern Alps should have been located within or south of the Adamello magmatic area. Exclusive volcanic debris of similar age arrived in the Trentino basin as indicated by the Plagioclase Arenites.

Table 2 Summary of published radiometric dating both in the Peri-Adriatic magmatic provenances and syn-sedimentary volcanic products in the Alpine orogen (*Zr* Zircon)

Rock type	Unit	Location	Age (Ma)	εHf	Lithology	Author	Mineral	Method
Intrusions	Adamello	Southern Re di Castello	42.0		Tonalite and granodiorite	Mayer et al. 2003	U/Pb Zr	SIMS
		Central part	37.0		Tonalite	Mayer et al. 2003	U/Pb Zr	SIMS
		Peripheral rims	31.0		Tonalite	Mayer et al. 2003	U/Pb Zr	SIMS
		southern Re di Castello	42.4–40.9	− 2.8 to + 8.9	Tonalite and granodiorite	Schaltegger et al. 2009	U/Pb Zr	LA-ICP-MS
		Whole area	43.7–33.1	− 10.0 to + 10.0	Tonalite and granodiorite	Skopelitis et al. 2011	U/Pb Zr	LA-ICP-MS
		Presanella pluton	33.9	− 7.5	Tonalite	Ji et al. 2013	U/Pb Zr	LA-ICP-MS
		Corno Alto and Re di Castello	43.2–43.0	+ 5.0 to + 7.7	Tonalite	Ji et al. 2013	U/Pb Zr	LA-ICP-MS
		Re di Castello	50.0–41.0	+ 7.0 to + 9.0	Hornblendite and amphibole gabbro	Tiepolo et al. 2014	U/Pb Zr	LA-ICP-MS
		Val Fredda	42.5	+ 2.0 to + 12.0	Gabbro to granodiorite	Broderick et al. 2015	U/Pb Zr	TIMS
	Bergell	Easternmost margin	31.9		Tonalite	von Blankenburg 1992	U/Pb Zr	TIMS
		Novate granite	26.6–21.6		Granite	Liati et al. 2000	U/Pb Zr	SHRIMP
		transition zone	31.2		Tonalite and granodiorite	Gianola et al. 2014	U/Pb Zr	LA-ICP-MS
		Val Sissone	33.8–28.0	+ 5.5 to + 1.7	Amphibole gabbro and diorite	Tiepolo et al. 2014	U/Pb Zr	LA-ICP-MS
		Central area	32.1–30.3	− 5.0 to − 3.2	Tonalite and granodiorite	Ji et al. 2013	U/Pb Zr	LA-ICP-MS
	Biella	Biella volcanic suite	32.9–32.4		Calc-alkaline lava	Kapferer et al. 2012	U/Pb Zr	LA-ICP-MS
		Valle del Cervo Pluton	30.4		Granitic core	Berger et al.2012	U/Pb Zr	LA-ICP-MS
		Miagliano Pluton	33.0		Tonalitic part	Berger et al. 2012	U/Pb Zr	LA-ICP-MS
		Biella volcanic suite	33.3–29.5		Trachyandesite	Scheuring et al. 1974	Hornblende	K/Ar
		Whole area	30.5–30.1	− 5.9 to − 1.8	Granitoid rock	Ji et al. 2013	U/Pb Zr	LA-ICP-MS
Sediments	Northern Alpine Foreland Basin	Alpe Taveyanne	31.7/32.4		Boulder in Taveyannaz Fm.	Fischer and Villa 1990	Hornblende	K/Ar
		Haute-Savoie	31.0/32.0		Boulder in Taveyannaz Fm.	Féraud et al. 1995	Hornblende	K/Ar
		Haute-Savoie	32.5		Boulder in Taveyannaz Fm.	Ruffini et al. 1997	Hornblende	K/Ar
	Southern Alps	Trentino basin	35.4		Plagioclase Arenite	Martin and Macera 2014	U/Pb Zr	LA-ICP-MS

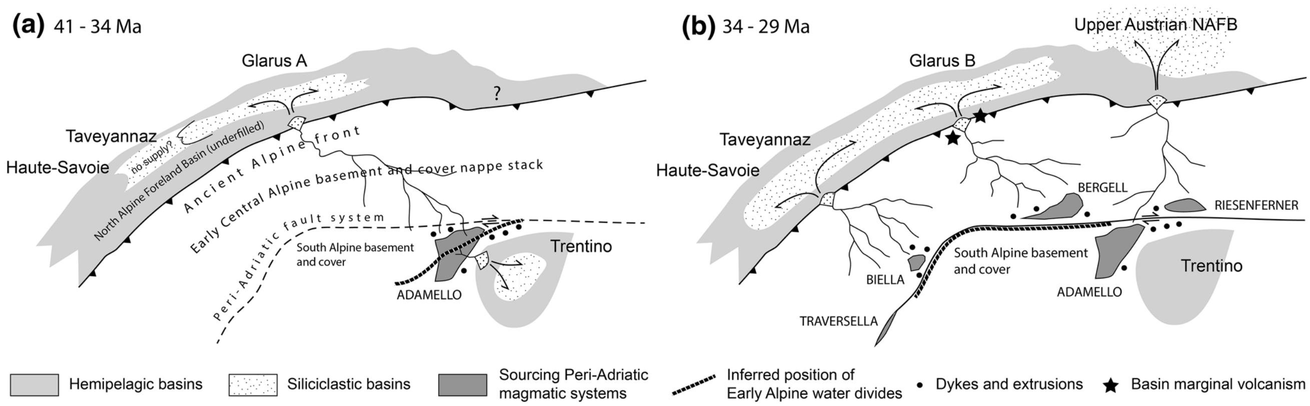

Fig. 10 Palaeogeographic reconstruction of the late Liddle Eocene—Early Oligocene Alpine source-to-sink systems. From 41 to 33 Ma the Glarus A and Trentino basin were supplied from the northern Adamello magmatic system. The absence of contemporaneous detrital zircons in the Haute-Savoie and Alpe Taveyanne areas possibly indicates prolonged hemipelagic sedimentation in that part of the North Alpine foreland basin. From 34 to 29 Ma the Glarus B and Haute-Savoie/Alpe Taveyanne were supplied from the Bergell and Biella magmatic systems, respectively

7.3.2 34–29 Ma (Rupelian, Fig. 10b)

According to the Cenozoic DZ supply at around 34 Ma a major palaeogeographical change in sediment routing and volcaniclastic sourcing should have occurred. In the western NAFB (Alpe Taveyanne and Haute-Savoie) turbidite fan deposition was initiated by volcaniclastic material originating from the Biella intrusion and volcaniclastic suite. More or less simultaneously, the Bergell magmatic system started to deliver volcanic material to the Glarus B basin of the NAFB. The Adamello source apparently disappeared in the sedimentary record of the northern Alpine foreland basin. Basement derived DZ continued to dominate but do not depict any trend across this age line. To explain this abrupt change in sediment routing we suggest a strong phase of right-lateral displacement and transpression along the Peri-Adriatic fault system. Consequently, the water divide was pushed north to a position coinciding with the present Insubric Line (Fig. 10b). This process made available sourcing in the Bergell magmatic system. Additional phreato-volcanic pebbles occur in the youngest, informal Ruchi sandstone member of the Taveyannaz Fm. of the Glarus area (Siegenthaler 1974). Because of their out-sized character and fragile composition we suggest that they were additionally supplied by volcanic eruptions along the southern margin of the NAFB, most likely near deltas from where the tubiditic flows initiated.

Detrital zircon age data from the NAFB in Upper Austria, accessed by drill holes, reveal in the informal "Rupelian Sandstone" a typical Adamello age population ($\sim$ 39–34 Ma, Sharman et al. 2017). Also there the Late Eocene DZ grains are intensely mixed with various old basement zircons. This may suggest that, in contrast to the Central Alps, the Adamello source continued supply to the eastern NAFB.

8 Conclusions

This study provides a thorough re-evaluation of the pertinent problem of the volcanic sources of the TF in the NAFB. Our conclusions are mainly based on DZ laser-ablation U–Pb dating and geochemical signatures of detrital zircons. Important correlation arguments also come from the investigation of coeval volcaniclastic sandstones in the Southern Alps (Trentino basin).

1. The sum of geochronological results suggests that the volcanic materials in the Taveyannaz Fm come from surficial extrusions and dykes along the Peri-Adriatic fault between 41 and 29 Ma.
2. By using the DZ age ranges as a stratigraphic correlation tool, the results confirm earlier results based on biostratigraphic dating. We suggest a longer, maximum age range for the Glarus TF (late Bartonian-Rupelian) than in the Alpe Taveyanne and Haute-Savoie sections (Rupelian).
3. The DZ ages and geochemical signatures allow to identify all in the reach lying Peri-Adriatic magmatic systems as suppliers to the NAFB, however, changing in time and space, due to palaeotectonic processes.
4. The presence of numerous Neo-Proterozoic and Palaeozoic DZ infers a mixture of the volcanic products with Alpine basement material, hence, common long-distance fluvial transport to the basin margins.
5. In an earlier stage (41–34 Ma), the Glarus A basin was supplied with volcanic debris from volcanic surface products related to the northern Adamello intrusion. Similar volcanic zircons in sandstones within the Southern Alps hemipelagic basins corroborate the origin. During this period the early Alpine water

divide was located somewhere within or south of the Adamello area. In the western part of the NAFB (Alpe Taveyanne and Haute-Savoie) presumably hemipelagic sedimentation maintained.

6. Around 34 Ma the earlier drainage divide migrated into a position close to the Palaeo-Insubric Line, as sugegsted by the coeval change of detrital supply to the NAFB. From 34 to 29 Ma in the Glarus B section an influx from the Bergell, and in the Alpe Taveyanne/Haute-Savoie from the synchronous Biella magmatic system is evident. The same volcaniclastic sources are continuously recorded in the overlying younger sandstone formations (Elm/Matt and Grés de Val d'Illiez fms.). Thus, the drastic change implies strong right-lateral transpressive movements along the Peri-Adriatic fault system, which created a barrier between the Southern and Northern Alps.
7. Because of re-sedimentation of fragile phreato-volcanic pebbles into the Glarus B basin, an additional contemporaneous volcanic source situated along the southern margin of the NAFB is implied.

Acknowledgements We thank G. Fellin, V. Picotti, P. Brack, A. Beltrán-Triviño, D. Letsch, A. Mohammadi for continuous advice in the lab and for numerous discussions, M. Guillong for the great support while acquiring the U/Pb and the Hf data, and A. Di Capua for the continued help during field work and sample analysis. The journal reviewers A. El Korh and J. Hermann are thanked for their numerous constructive comments and suggestions. The support by a Chinese Scholarship (CSC) and ETH internal funding is much appreciated.

Appendix 1

Detrital zircons were extracted from ~ 5 kg rock samples by applying standard mechanical mineral separation techniques. Samples were crushed into small fragments (< 1 mm) and sieved to 400–63 µm. Heavy mineral and magnetic separation followed standard procedures in the lab: A Frantz magnet separator was used to separate magnetic from non-magnetic minerals. Methylene iodide ($d = 3.32$ g/cm^3) served for density separation. Zircon grains were picked from the heavy mineral concentrates. Prior to isotopic analyses, all zircon grains were inspected by cathodoluminescence imaging to check for homogeneous composition and their magmatic growth pattern. Laser ablation ICP-MS U–Pb dating of detrital zircon was performed in a spot mode of 30 µm diameter using an Excimer laser (ArF 193 nm, Resonetics resolution 155) coupled to a PE SCIEX Elan 6100 ICP-MS in the Institute of Isotope Geochemistry and Petrology (IGP), ETH Zurich (Guillong et al. 2014; von Quadt et al. 2014). A gas-stream was used to transport the ablated material (He, flux rate 1.1 l/s). The laser pulse repetition rate was 5 Hz and energy density/fluence was ~ 2.0 J cm^{-2}. The elements (Pb, U, Th) have been detected with 10 ms (202Hg, 204Pb, 202Hg is measured to monitor Hg interference on mass 204. 204Pb is measured to monitor and avoid common Pb-rich domains.), 20 ms (208Pb, 232Th, 235U, 238U) and 40 ms (206Pb, 207Pb) dwell time and 3 ms quadrupole settling time.

Backgrounds were measured for 30 s and ablation duration was about 40 s. The accuracy and reproducibility of U–Pb zircon analyses were monitored by periodic measurements of the external standard (AUSZ7-5, Plesovice, Temora2, 91,500, NIST610; von Quadt et al. 2014). GJ-1 is used as a primary reference standard and NIST 610 to calculate the trace element composition. There are consistent with the theoretical age. Limits of detection are calculated as 3 times the standard deviation of the background normalised to the volume of the ablated sample (cps/µg/g). ^{207}Pb/^{206}Pb, ^{206}Pb/^{238}U, ^{207}Pb/^{235}U, and ^{208}Pb/^{232}Th ratios and ages were calculated using IOLITE 2.5 (Paton et al. 2011; Petrus and Kamber, 2012). Calculated isotopic ratios and ages were processed with ISOPLOT 4.0 (Toolkit for Microsoft Excel; Ludwig 2012) to constrain concordia plots and frequency U–Pb age distribution diagrams. In this study, only concordant ages are considered for calculation, although occasionally those small-margin-error ellipses situated close and only below the concordant age curve are taken into account if the error is not higher than 2-sigma. Trace element concentrations (P, Y, Th, U, Pb, Nb, Ta, REE and Hf) on the dated detrital zircons were measured and analyzed to determine the igneous rock type in which grains had crystallized (CART Tree method; Belousova et al., 2002).

In-situ Hf isotope analysis was carried out using a 193 nm ArF laser connected to a Nu3 MC-ICP-MS. Ablation was carried using He as a sweep gas with a flow rate of ~ 0.9 l/min and combined with Ar (~ 0.7 l/min) using a 40 um spot size and a 5 Hz laser pulse repetition rate. The baseline was measured within 30 s and ablated zircon within 60 s.

Lutetium and Yb were analysed inorder to correct for isobaric interferences on ^{176}Hf using ^{173}Yb/^{176}Yb = 0.79618 and ^{175}Lu/^{176}Lu = 0.026549 (Chu et al. 2002). The Hf and Yb mass bias coefficients were calculated using an exponential law from measured ^{176}Hf/^{177}Hf and ^{173}Yb/^{176}Yb respectively and using natural abundance reference values (^{176}Hf/^{177}Hf = 0.7325; ^{173}Yb/^{176}Yb = 1.132685; Chu et al. 2002). The Lu mass bias fractionation was assumed to be the same as Yb. The accuracy and precision of the data obtained was monitored through the systematic measurements of the well characterized Temora-2 (0.282686; Woodhead and Hergt 2005). Mud Tank (0.282507; Woodhead and Hergt 2005) and

Plesovice (0.282482; Sláma et al. 2008) reference natural zircon samples with known Hf isotopic compositions. The standard reference materials were chosen in order to have a range in Yb/Hf ratios to test the accuracy of the ^{176}Yb correction following the protocols of Fisher et al. (2014). Repeated standard analysis yielded results for the analytical session: Temora-2 = 0.282683, n = 37; Plesovice 0.282474, n = 17; Mud Tank = 0.282494, n = 21, which are good agreement with the published values. Throughout the sample session initial ^{176}Hf/^{177}Hf ratios and εHf were calculated using an age of 7.1 Ma and the CHUR parameters of Bouvier et al. (2008). All uncertainties are reported at the 2-sigma level.

References

Allen, P. A., Crampton, S. L., & Sinclair, H. D. (1991). The inception and early evolution of the North Alpine Foreland Basin, Switzerland. *Basin Research, 3,* 143–163.

Bars, H., & Grigoriades, J. (1969). Über Basalttuffite der oberen Mittel-Eozäns der Scaglia Grigia im Val di Non (Nonsberg), Provinz Trient, Italien. *Neues Jahrbuch Geologie Paläontologie, Monatsheft, 1969,* 643–645.

Belousova, E., Griffin, W. L., O'Reilly, S. Y., & Fisher, N. L. (2002). Igneous zircon: trace element composition as an indicator of source rock type. *Contributions to Mineralogy and Petrology, 143,* 602–622.

Beltrando, M., Lister, G. S., Rosenbaum, G., Richards, S., & Forster, M. A. (2010). Recognizing episodic lithospheric thinning along a convergent plate margin: The example of the Early Oligocene Alps. *Earth-Science Reviews, 103,* 81–98.

Beltrán-Triviño, A., Winkler, W., von Quadt, A., & Gallhofer, D. (2016). Triassic magmatism on the transition from Variscan to Alpine cycles: evidence from U-Pb, Hf, and geochemistry of detrital minerals. *Swiss Journal of Geosciences, 109,* 309–328.

Beltràn-Triviño, A., Winkler, W., & von Quadt, A. (2013). Tracing Alpine sediment sources through laser-ablation U-Pb dating and Hf-isotopes of detrital zircons. *Sedimentology, 60,* 197–224.

Berger, A., Mercolli, I., Kapferer, N., & Fügenschuh, B. (2012). Single and double exhumation of fault blocks in the internal Sesia-Lanzo Zone and the Ivrea-Verbano Zone (Biella, Italy). *International Journal of Earth Sciences, 101,* 1877–1894.

Bouvier, A., Vervoort, J. D., & Patchett, P. J. (2008). The Lu–Hf and Sm–Nd isotopic composition of CHUR: Constraints from unequilibrated chondrites and implications for the bulk composition of terrestrial planets. *Earth and Planetary Science Letters, 273,* 48–57.

Boyet, M., Lapierre, H., Tardy, M., Bosch, D., & Maury, R. (2001). Nature des sources des composantes andésitiques des Grés du Chaupsaur et des Grés de Taveyannaz. Implications dans l'evolution des Alpes occidentales au Paléogène. *Bulletin Société géologique de France, 172,* 487–501.

Broderick, C., Wotzlaw, J. F., Frick, D. A., Gerdes, A., Ulianov, A., Günther, D., et al. (2015). Linking the thermal evolution and emplacement history of an upper-crustal pluton to its lower-crustal roots using zircon geochronology and geochemistry (southern Adamello batholith, N. Italy). *Contributions to Mineralogy and Petrology, 170,* 28.

Bütler, E., Winkler, W., & Guillong, M. (2011). Laser ablation U/Pb age patterns of detrital zircons in the Late Maatrichtian—Early Eocene Schlieren flysch (Central Switzerland): New proves on the detrital sources. *Swiss Journal of Geoscience, 104,* 225–236.

Callegari, E., & Brack, P. (2002). *Geological map of the Tertiary Adamello batholith (northern Italy): Explanatory notes and legend*. Tipografica: Società Coop.

Callegari, E., Cigolini, C., Medeot, O., & D'Antonio, M. (2004). Petrogenesis of calc-alkaline and shoshonitic post-collisional Oligocene volcanics of the Cover Series of the Sesia Zone, Western Italian Alps. *Geodinamica Acta, 17,* 1–29.

Castellarin, A., Dal Piaz, G. V., Picotti, V., Selli, L., Cantelli, L., Martin, S., et al. (2005). *Carta Geologica d'Italia, 1:50 000, 059 Tione di Trento, mit Erläuterungen*. Rom: APAT.

Chu, N. C., Taylor, R. N., Chavagnac, V., Nesbitt, R. W., Boella, R. M., Milton, J. A., et al. (2002). Hf isotope ratio analysis using multi-collector inductively coupled plasma mass spectrometry: an evaluation of isobaric interference corrections. *Journal of Analytical Atomic Spectrometry, 17,* 1567–1574.

DeCelles, P. G., & Giles, K. A. (1996). Foreland basin systems. *Basin Research, 8,* 105–123.

Di Capua, A., & Groppelli, G. (2015). Application of actualistic models to unravel primary volcanic control on sedimentation (Taveyanne Sandstones, Oligocene Northalpine Foreland Basin). *Sedimentary Geology, 336,* 147–160.

Doglioni, C., & Bosellini, A. (1987). Eoalpine and mesoalpine tectonics in the Southern Alps. *Geologische Rundschau, 76,* 735–754.

Féraud, G., Ruffet, G., Stéphan, J. F., Lapierre, H., Delgado, E., & Popoff, M. (1995). Nouvelles données géochronologiques sur le volcanisme paléogène des Alpes occidentales: existence d'un événement magmatique bref généralisé. *Séance Spéciale de la Société géologique de France et de l" Association des Géologues du SE" Magmatismes dans le sud-est de la France",* Nice (pp. 25–26).

Ferrero Mählmann, R. (1995). Das Diagenese-Metamorphose-Muster von Vitrinitreflexion und Illit-„Kristallinität"in Mittelbünden und im Oberhalbstein. Teil 1: Bezüge zur Stockwerktektonik. *Schweizerische Mineralogische Petrographische Mitteilungen, 75,* 85–122.

Fischer, H., & Villa, I. M. (1990). Erste Ar/Ar und Ar/Ar-Hornblende-Mineralalter des Taveyannaz-Sndsteins. *Schweiz Mineral Petrograph Mitteilungen, 70,* 73–75.

Fisher, C. M., Vervoort, J. D., & Hanchar, J. M. (2014). Guidelines for reporting zircon Hf isotopic data by LA-MC-ICPMS and potential pitfalls in the interpretation of these data. *Chemical Geology, 363,* 125–133.

Fontignie, D., Delaloye, M., & Bertrand, J. (1982). Ages radiometriques K/Ar des elements ophiolitiques de la nappe des Gets (Haute-Savoie, France). *Eclogae geologicae Helvetiae, 75,* 117–126.

Ford, M., & Lickorish, W. H. (2004). *Foreland basin evolution around the western Alpine Arc* (pp. 39–63). London: Geological Society.

Frisch, W., Neubauer, F., & Satir, M. (1984). Concepts of the evolution of the Austroalpine basement complex (Eastern Alps) during the Caledonian-Variscan cycle. *Geologische Rundschau, 73,* 47–68.

Furrer, H., & Hügi, Th. (1952). Telemagmatischer Gang im Nummulitenkalk bei Trubeln westlich Leukerbad (Kanton Wallis). *Eclogae Geologicae Helvetiae, 45,* 41–51.

Gehrels, G. (2014). Detrital zircon U-Pb geochronology applied to tectonics. *Annual Review of Earth and Planetary Sciences, 42,* 127–149.

Gianola, O., Schmidt, M. W., von Quadt, A., Peytcheva, I., Luraschi, P., & Reusser, E. (2014). Continuity in geochemistry and time of the Tertiary Bergell intrusion (Central Alps). *Swiss Journal of Geosciences, 107,* 197–222.

Gifkins, C. C., Herrmann, W., & Large, R. R. (2005). *Altered Volcanic Rocks. A guide to description and interpretation* (p. 274). Hobart: Centre for Ore Deposit Research University of Tasmania.

Gradstein, F. M., Ogg, J. G., Schmitz, M., & Ogg, G. (Eds.). (2012). *The geologic time scale 2012* (p. 1176). Amsterdam: Elsevier.

Guillong, M., von Quadt, A., Sakata, S., Peytcheva, I., & Bachmann, O. (2014). LA-ICP-MS Pb–U dating of young zircons from the Kos-Nisyros volcanic centre, SE Aegean arc. *Journal of Analytical Atomic Spectrometry, 29,* 963–970.

Hawkesworth, C. J., & Kemp, A. I. S. (2006). Using hafnium and oxygen isotopes in zircons to unravel the record of crustal evolution. *Chemical Geology, 226,* 144–162.

Ji, W. Q., Wu, F. Y., Tiepolo, M., Langone, A., & Braga, A. (2013). Zircon U-Pb age and Hf isotope constraints on the petrogenesis of the Alpine Peri-Adriatic intrusions. *Mineralogical Magazine, 77,* 1386.

Kapferer, N., Mercolli, I., Berger, A., Ovtcharova, M., & Fügenschuh, B. (2012). Dating emplacement and evolution of the orogenic magmatism in the internal Western Alps: 2. The Biella Volcanic Suite. *Swiss Journal of Geosciences, 105,* 67–84.

Lateltin, O. (1988). Les dépôts turbiditiques oligocènes d'avant-pays entre Annecy (Haute-Savoie) et le Sanetsch (Suisse). *Ph.D. Theise,* Fribourg University, Switzerland, p. 127.

Lateltin, O., & Muller, D. (1987). Evolution paléogéographique du bassin des grès de Taveyannaz dans les Aravis (Haute-savoie) à la fin du Paléogène. *Eclogae Geologicae Helvetiae, 80,* 127–140.

Letsch, D., Winkler, W., von Quadt, A., & Gallhofer, D. (2015). The volcano-sedimentary evolution of a post-Variscan intramontane basin in the Swiss Alps (Glarus Verrucano) as revealed by zircon U-Pb age dating and Hf isotope geochemistry. *International Journal of Earth Sciences, 104,* 123–145.

Liati, A., Gebauer, D., & Fanning, M. (2000). U-Pb SHRIMP dating of zircon from the Novate Granite (Bergell, Central Alps); evidence for Oligocene-Miocene magmatism, Jurassic/Cretaceous continental rifting and opening of the Valais Trough. *Schweizerische mineralogische und petrographische Mitteilungen, 80,* 305–316.

Ludwig, K. R. (2012). *User's manual for Isoplot 3.75: A geochronological toolkit for Microsoft Excel* (p. 75). Berkeley: Geochronology Center Special Publication.

Martin, S., & Macera, P. (2014). Tertiary volcanism in the Italian Alps (Giudicarie fault zone, NE Italy): Insight for double alpine magmatic arc. *Italian Journal of Geosciences, 133,* 63–84.

Mayer, A., Cortiana, G., Dal Piaz, G. V., Deloule, E., De Pieri, R., & Jobstraibitzer, P. (2003). U-Pb single zircon ages of the Adamello batholith, Southern Alps. *Memoir di Scienze Geologiche (Padova), 55,* 151–167.

McDonough, W. F., & Sun, S. S. (1995). The composition of the Earth. *Chemical Geology, 120,* 223–253.

Paton, C., Hellstrom, J., Paul, B., Woodhead, J., & Hergt, J. (2011). Iolite: Freeware for the visualisation and processing of mass spectrometric data. *Journal of Analytical Atomic Spectrometry, 26,* 2508–2518.

Petrus, J. A., & Kamber, B. S. (2012). VizualAge: A novel approach to laser ablation ICP-MS U-Pb geochronology data reduction. *Geostandards and Geoanalytical Research, 36,* 247–270.

Pfiffner, A. O. (1986). Evolution of the north Alpine foreland basin in the Central Alps. *Special Publication International Association Sedimentology, 8,* 219–228.

Pfiffner, A. Q. (2014). *Geology of the Alps* (pp. 140–165). West Sussex: Wiley.

Rahn. M. (1994). Incipient metamorphism of the Glarus Alps: petrology of the Taveyanne greywacke and fission track dating. *Unpubl. Ph.D. Thesis,* University of Basel, Switzerland, p. 209.

Rahn, M., Stern, W. B., & Frey, M. (1995). The origin of the NH Flysch: arguments from whole-rock and clinopyroxene composition. *Schweizerische Mineralogische Petrographische Mitteilungen, 75,* 213–224.

Rosenberg, C. L. (2004). Shear zones and magma ascent: a model based on a review of the Tertiary magmatism in the Alps. *Tectonics*, 23, 1–21.

Rossetti, P., Agangi, A., Castelli, D., Padoan, M., & Ruffini, R. (2007). The Oligocene Biella pluton (western Alps, Italy): new insights on the magmatic vs. hydrothermal activity in the Valsessera roof zone. *Periodico di Mineralogia, 76,* 223–240.

Rubatto, D., & Gebauer, D. (2000). Use of cathodoluminescence for U-Pb Zircon dating by ion microprobe: some examples from the Western Alps. In M. Pagel, Ph Blanc, V. Barbin, & D. Ohnenstetter (Eds.), *Cathodoluminescence in Geosciences* (pp. 373–400). Berlin, Heidelberg: Springer.

Rubatto, D., & Hermann, J. (2003). Zircon formation during fluid circulation in eclogites (Monviso, Western Alps): implications for Zr and Hf budget in subduction zones. *Geochimica et Cosmochimica Acta, 67,* 2173–2187.

Ruffini, R., Polino, R., Calegari, E., Hunziker, L. C., & Pfeiffer, H. R. (1997). Volcanic clast rich turbidites of the Taveyanne sandstone from the Thônes syncline (Savoie, France): records for a Tertiary postcollisional volcanism. *Schweizerische Mineralogische und Petrographische Mitteilungen, 77,* 161–174.

Schaltegger, U., Brack, P., Ovtcharova, M., Peytcheva, I., Schoene, B., Stracke, A., et al. (2009). Zircon and titanite recording 1.5 million years of magma accretion, crystallization and initial cooling in a composite pluton (southern Adamello batholith, northern Italy). *Earth and Planetary Science Letters, 286,* 208–218.

Scheuring, B., Ahrendt, H., Hunziker, J. C., & Zingg, A. (1974). A Tertiary Andesite Complex NW Biella on the Boundary between central and southern Alps. *Geology Rdsch, 63,* 305–325.

Schoene, B., Schaltegger, U., Brack, P., Latkoczy, Ch., Stracke, A., & Günther, D. (2012). Rates of magma differentiation and emplacement in a ballooning pluton recorded by U-Pb TIMS-TEA, Adamello batholith, Italy. *Earth and Planetary Science Letters, 355–356,* 162–173.

Sciunnach, D., & Borsato, A. (1994). Plagioclase-arenites in the Molveno Lake area (Trento): record of an Eocene volcanic arc. *Studi Trentini di Scienze Naturali, 69,* 81–92.

Shanks, III., W. C. Pat, (2012). Hydrothermal alteration in volcanogenic massive sulfide occurrence model. U.S. Geological Survey Scientific Investigations Report 2010–5070–C, Chap. 11, p. 12.

Sharman, G. R., Hubbard, S. M., Covault, J. A., Hinsch, R., Linzer, H.-G., & Graham, S. A. (2017). Sediment routing evolution in the North Alpine foreland basin, Austria: Interplay of transverse and longitudinal sediment dispersal. *Basin Research*. https://doi.org/10.1111/bre.12259.

Siegenthaler, C. (1974). Die Nordhelvetische Flysch-Gruppe im Sernftal (Kt. Glarus). *Doctoral dissertation*, Geologisches Institut der Eidg. Technischen Hochschule und der Universität Zürich, p. 83.

Sinclair, H. D. (1992). Turbidite sedimentation during Alpine thrusting: The NH Flyschs of eastern Switzerland. *Sedimentology, 39*(5), 837–856.

Sinclair, H. D., & Tomasso, M. (2002). Depositional evolution of confined turbidite basins. *Journal of Sedimentary Research, 72,* 451–456.

Skopelitis, A. (2014). Formation of a tonalitic batholith through sequential accretion of magma batches. *Unpubl. Ph.D. Thesis*, Geneva University, Switzerland, p. 328.

Skopelitis A., Brack P., Ulianov A., Bindeman I., & Schaltegger U. (2011). Tracing episodic magma accretion by zircon 18O/16O isotopes and U-Pb dating in the Adamello batholith, Italy. *Goldschmidt Conference,* 14–19. 8. 2011, Prague.

Sláma, J., Košler, J., Condon, D. J., Crowley, J. L., Gerdes, A., Hanchar, J. M., et al. (2008). Plešovice zircon-a new natural reference material for U-Pb and Hf isotopic microanalysis. *Chemical Geology, 249,* 1–35.

Stern, R. J., Johnson, P. R., Kröner, A., & Yibas, B. (2004). Neoproterozoic ophiolites of the Arabian-Nubian shield. *Developments in Precambrian Geology, 13,* 95–128.

Stipp, Michael, Nommensen, L., Münker, C., Pomella, H., & Fügenschuh, B. (2013). New constraints on kinematics and timing of the Periadriatic Fault System from the petrology and Lu-Hf apatite geochronology of Giudicarian magmatic lamellae and the Presanella intrusion (Southern Alps, Italy). *11. Workshop on Alpine Geological Studies,* 07-14.09.2013, Schladming, Austria.

Tiepolo, M., Tribuzio, R., Ji, W. Q., Wu, F. Y., & Lustrino, M. (2014). Alpine Tethys closure as revealed by amphibole-rich mafic and ultramafic rocks from the Adamello and the Bergell intrusions (Central Alps). *Journal of the Geological Society, 171,* 793–799.

Trümpy, R. (1973). The timing of orogenic events in the Central Alps. In De Jong, K.A., & Schollen, R. (Eds.), *Gravity and tectonics* (pp. 229–251). New York: Wiley.

von Blanckenburg, F., & Davies, J. H. (1995). Slab breakoff: A model for syncollisional magmatism and tectonics in the Alps. *Tectonics, 14,* 120–131.

von Blankenburg, F. (1992). Combined high-precision chronometry and geochemical tracing using accessory minerals: applied to the Central-Alpine Bergell intrusion (central Europe). *Chemical Geology, 100,* 19–40.

von Quadt, A., Gallhofer, D., Guillong, M., Peytcheva, I., Waelle, M., & Sakata, S. (2014). U/Pb dating of CA/non-CA treated zircons obtained by LA-ICP-MS and CA-TIMS techniques: impact for their geological interpretation. *Journal of Analytical Atomic Spectrometry, 29,* 1618–1629.

von Raumer, J. F., Bussy, F., Schaltegger, U., Schulz, B., & Stampfli, G. M. (2013). Pre-Mesozoic Alpine basements—their place in the European Paleozoic framework. *Geological Society of America Bulletin, 125,* 89–108.

Vuagnat M. (1944). Essai de subdivision à l'intérieur des grès de Taveyannaz grès d'Aldorf. *Eclogae geologicae Helvetiae, 37,* 427–430.

Waibel, A. F. (1993). Nature and plate-tectonic significance of orogenic magmatism in the European Alps: a review. *Schweizerische Mineralogische und Petrographische Mitteilungen, 73,* 391–405.

Woodhead, J. D., & Hergt, J. M. (2005). A preliminary appraisal of seven natural zircon reference materials for in situ Hf isotope determination. *Geostandards and Geoanalytical Research, 29,* 183–195.

Zurfluh, R. (2012). Eozäne vulkanoklastische Sandsteine im Nonsberg/Italien. Unpubl. BSc Thesis, ETH Zurich, Switzerland, p. 33.